character of band c is not expected to change upon the layer stacking of **4b**. As a result, the energy gap between band a at $Z$ in Figure 2b and band c at $\Gamma$ in Figure 2a is expected to remain even if the layer stacking **4b** is taken into consideration. In agreement with this expectation, $Li_{0.33}MoO_3$ is found to be semiconducting in all directions.[12] Since the valence and the conduction bands of Figure 2 are dispersive along $\Gamma \rightarrow Z$, the electrical conductivity of $Li_{0.33}MoO_3$ is expected to be largest along the $c$ direction.

### Concluding Remarks

In crystal structure, $Li_{0.33}MoO_3$ differs from other alkali-metal bronzes with the same composition $A_{0.33}MoO_3$ (A = K, Cs, Tl), although it is made up of the same building block, $MoO_6$ octahedra. By recognizing how the $t_{2g}$-level degeneracy of a regular $MoO_6$ octahedron is lifted upon distortion, it is possible to deduce the nature of the bottom d-block bands of $Li_{0.33}MoO_3$, just on the basis of the tight-binding band electronic structures of the $Mo_6O_{24}$ chains that constitute $Li_{0.33}MoO_3$. The present analysis suggests $Li_{0.33}MoO_3$ to be a small band gap semiconductor, which is consistent with the available resistivity data on $Li_{0.33}MoO_3$.

**Acknowledgment.** This work was supported by NATO, Scientific Affairs Division, and also by DOE, Office of Basic Sciences, Division of Materials Science, under Grant DE-FG05-86-ER45259. M.-H.W. thanks Prof. M. Greenblatt for communication of results prior to publication.

**Registry No.** $Li_{0.33}MoO_3$, 111556-63-9.

---

Contribution from the Department of Chemistry, Oregon State University, Corvallis, Oregon 97331, and Isotopes and Nuclear Chemistry Division, Los Alamos National Laboratory, Los Alamos, New Mexico 87545

# Dioxygen Difluoride: Electron Diffraction Investigation of the Molecular Structure in the Gas

Lise Hedberg,[†] Kenneth Hedberg,*[†] P. G. Eller,[‡] and R. R. Ryan[‡]

*Received July 27, 1987*

An electron diffraction study of the structure of dioxygen difluoride ($O_2F_2$) at −42 °C has confirmed the results of an earlier microwave investigation. The molecule has $C_2$ symmetry, a short O–O bond, and extraordinarily long O–F bonds: $r_g$(O–O) = 1.216 (2) Å, $r_g$(O–F) = 1.586 (2) Å. Other parameter values are $\angle_a$FOO = 109.2 (2)°, $\angle_a$FOOF = 88.1 (4)°, $l$(O–O) = 0.046 (3) Å, $l$(O–F) = 0.069 (3) Å, $l$(O···F) = 0.073 (4) Å, and $l$(F···F) = 0.113 (10) Å; the $l$ values are rms amplitudes of vibration, and the parameter uncertainties are estimated $2\sigma$. The data are consistent with a high barrier to internal rotation. There is no evidence for the presence of a planar form. Attempts to detect $O_2F$ radical or its dimer were unsuccessful.

### Introduction

For some time dioxygen difluoride, hereafter $O_2F_2$, has been recognized as one of the most potent of all molecular oxidative fluorinating agents.[1] Several years ago it was discovered that $O_2F_2$ can convert substrates of the actinides U, Np, and Pu to their volatile hexafluorides at effective rates near or below room temperature, i.e. at temperatures 300–400 °C *lower* than those required with any other molecular agents except $KrF_2$.[2,3] This discovery has important consequences for a number of aspects of nuclear processing and has led to fundamental studies of the properties of $O_2F_2$.[2,3] The temperature advantage also has significant implications for synthesis of other high-valent, thermally unstable main-group and metallic fluorides.[4]

The structure of $O_2F_2$ is obviously of considerable interest in connection with its unusual oxidizing properties. A microwave investigation[5] showed the molecule to have a hydrogen peroxide like configuration with a dihedral angle of 87.5°, remarkably long O–F bonds (1.575 Å) compared to those in $OF_2$ (1.409 Å),[6] and a remarkably short O–O distance—at 1.217 Å only 0.010 Å greater than in dioxygen.[7] The vibrational spectrum of the molecule has been studied many times, and it now appears that uncertainties about some of the assignments[3,8-12] have been removed.[12] Theoretical interest in the molecule has also been stimulated by its unusual structure, but it has been very difficult to predict the observed geometry from quantum-mechanical calculations[13-16] to the accuracy one has come to expect for simple molecules.

Although the geometry of $O_2F_2$ seemed to have been securely established by the microwave work, the puzzling discrepancy between the microwave results and those from the theoretical calculations merited an additional experimental check by gas-phase electron diffraction. We also wished to investigate the possible presence of an anti form of the molecule and to attempt to obtain diffraction data for the dioxygen fluoride radical $O_2F$ (which results from decomposition of $O_2F_2$) and for the dimer of the radical, $O_4F_2$. The $O_2F$ radical is a well-documented species with a long gas-phase lifetime. The dimer has been reported to decompose at low temperature in the condensed phase to give $O_2F_2$ and $O_2$.[1]

### Experimental Section

Dioxygen difluoride was prepared at Los Alamos[2] and transported to Oregon State in stainless steel cans at liquid-nitrogen temperature for the

[†] Oregon State University.
[‡] Los Alamos National Laboratory.

(1) Streng, A. G. *Chem. Rev.* **1963**, *63*, 607.
(2) Malm, J. G.; Eller, P. G.; Asprey, L. B. *J. Am. Chem. Soc.* **1984**, *106*, 2726. Asprey, L. B.; Eller, P. G.; Kinkead, S. A.; Kissane, R. J.; Foltyn, E. M., submitted for publication in *Inorg. Synth.* Asprey, L. B.; Eller, P. G.; Kinkead, S. A. *Inorg. Chem.* **1986**, *25*, 670. Asprey, L. B.; Kinkead, S. A.; Eller, P. G. *Nucl. Technol.* **1986**, *73*, 69.
(3) Kim, K. C.; Campbell, G. M. *J. Mol. Struct.* **1985**, *129*, 263. Kim, K. C.; Campbell, G. M. *Chem. Phys. Lett.* **1985**, *116*, 236.
(4) Kinkead, S. A.; Asprey, L. B.; Eller, P. G. *J. Fluorine Chem.* **1985**, *29*, 459.
(5) Jackson, R. H. *J. Chem. Soc.* **1962**, 4585.
(6) Morino, Y.; Saito, S. *J. Mol. Spectrosc.* **1966**, *19*, 435.
(7) Huber, K. P.; Herzberg, G. *Molecular Spectra and Molecular Structure*; Van Nostrand: New York, 1979; Vol. IV.
(8) Spratley, R. D.; Turner, J. J.; Pimentel, G. C. *J. Chem. Phys.* **1966**, *44*, 2063.
(9) Loos, K. R.; Goetschel, C. T.; Campanile, V. A. *J. Chem. Phys.* **1970**, *52*, 4418.
(10) Burdett, J. K.; Gardiner, D. J.; Turner, J. J.; Spratley, R. D.; Tchir, P. *J. Chem. Soc., Dalton Trans.* **1973**, 1928.
(11) Jacox, M. E. *J. Mol. Spectrosc.* **1980**, *84*, 74.
(12) Woodruff, W. W.; Larson, E. M.; Swanson, B. I.; Kinkead, S. A.; Jones, L. H.; Eller, P. G.; Kissane, R. J., to be submitted for publication.
(13) Lucchese, R. R.; Schaefer, H. F., III; Rodwell, W. R.; Radom, L. *J. Chem. Phys.* **1978**, *68*, 2507.
(14) Ahlrichs, R.; Taylor, P. R. *Chem. Phys.* **1982**, *72*, 287.
(15) Clabo, D. A., Jr.; Schaefer, H. F., III *Int. J. Quantum Chem.* **1987**, *31*, 429.
(16) Rohlfing, C. M.; Hay, P. J. *J. Chem. Phys.* **1987**, *86*, 4518.

0020-1669/88/1327-0232$01.50/0 

diffraction experiments. *Caution*! $O_2F_2$ is one of the most powerful of all known oxidative fluorinating agents and can initiate extremely violent reactions. It also undergoes very rapid homogeneous decomposition at room temperature to form elemental fluorine and oxygen, with a corresponding pressure increase.

The sample bombs were attached to the Monel gas nozzle of the diffraction apparatus with Swagelok fittings. The inlet system was seasoned by passing sample through it for several minutes before each diffraction experiment. The vapor pressure of the samples was maintained at 4–10 Torr by slightly raising or lowering the liquid-nitrogen bath in which the cans were immersed. The residence time of the sample is estimated to have been less than 0.1 s in the nozzle portion of the system and about 1.5 s in the transfer line. The procedures for the collection of diffraction data and for extraction of the data from the photographic plates have been described.[17,18] The plates were made with an $r^3$ sector, accelerating potentials of 44.5 kV, and nozzle-to-plate distances of 75 and 30 cm and were developed for 10 min in D-19 developer diluted 1:1. The ambient pressure in the apparatus during sample run-in was $(1–3) \times 10^{-5}$ Torr.

Several experiments were carried out with conditions and results as follows. In all runs the transfer line was cooled with dry ice.

**Runs 1, 2, and 4.** The nozzle was maintained at −42 °C in order to obtain data for as nearly pure $O_2F_2$ as possible. These runs were successful.

**Run 3.** The nozzle was at 100 °C; the hope was that the high temperature might generate detectable amounts of the anti form of $O_2F_2$ and, because of the short residence time, the sample would escape the heated area after only partial decomposition. The results indicated, however, that essentially complete decomposition to $O_2$ and $F_2$ had occurred.

**Run 5.** The $O_2F_2$ can was warmed until pressures of 10–20 Torr were achieved, and then a very large excess of flowing $O_2$ was used to "carry" the $O_2F_2$ to a liquid-nitrogen-cooled trap. Volatiles were pumped away as the trap was slowly warmed, and when a relatively steady state pressure of $O_xF_y$ was obtained, the gas was admitted to the diffraction chamber. Analysis of the diffraction patterns showed this gas to be predominantly $O_2F_2$.

**Run 6.** Conditions were as in run 1 except that an equal pressure of $O_2$ was used to "carry" the $O_2F_2$ from the cooled $O_2F_2$ can into the diffraction unit in the hope of forming $O_2F$. However, analysis of the diffraction pattern of this sample indicated the gas to be about 49% $O_2F_2$ and about 48% $O_2$. When the oxygen flow was terminated, however, the residual $O_2$-carried $O_2F_2$ in the can did not give normal pressure behavior as in previous runs until the can had been pumped for a short time. This result was taken to indicate that either a compound with a different vapor pressure (e.g., $O_4F_2$), a solution of $O_2$ in $O_2F_2$, or an equilibrium of some sort (e.g., $O_2$ + FOOF = $F_2O_4$) existed. This point was not investigated further.

**Run 7.** Dioxygen difluoride was volatilized from the can as in runs 1, 2, and 4 and mixed with an equal pressure of $O_2$ in the transfer tube at room temperature before injection into the diffraction unit. The diffraction patterns gave evidence only for diatomic molecules in the sample. In this experiment it was found that the pressures were *not* additive, possibly indicative of reaction. However, there were uncertainties about the extent of gas mixing and about the flow rates that make it difficult to interpret these results.

Of the foregoing experiments, only runs 1, 2, and 4 yielded data that merited analysis for structure and composition. The plates from runs 1 and 2 were similar; those from run 1 were light and were not used. Five plates from the longer distance (run 4) and four from the shorter (run 2) were selected and yielded data over the ranges $2.00 \le s/\text{Å}^{-1} \le 13.75$ (longer distance) and $6.00 \le s/\text{Å}^{-1} \le 33.75$ (shorter distance). Curves of the data are shown in Figure 1. The final experimental radial distribution curve, calculated from the $sI_m(s)$ intensities after multiplication with $Z_FZ_OA_F^{-1}A_O^{-1}$ exp(−0.0025), is shown in Figure 2. Electron scattering amplitudes and phases used in these and later calculations were taken from ref 19. The intensity data are available as supplementary material.

## $O_2F_2$: Structure Analysis

**Quadratic Force Field.** The radial distribution curves indicated interatomic distanes that were in very good agreement with those deduced from the parameters of the microwave investigation,[5] and accordingly we decided to base our refinements of the structure on joint use of the rotational constants and the diffraction data. Such refinements are usually done in terms of $r_\alpha^0 = r_z$ distances

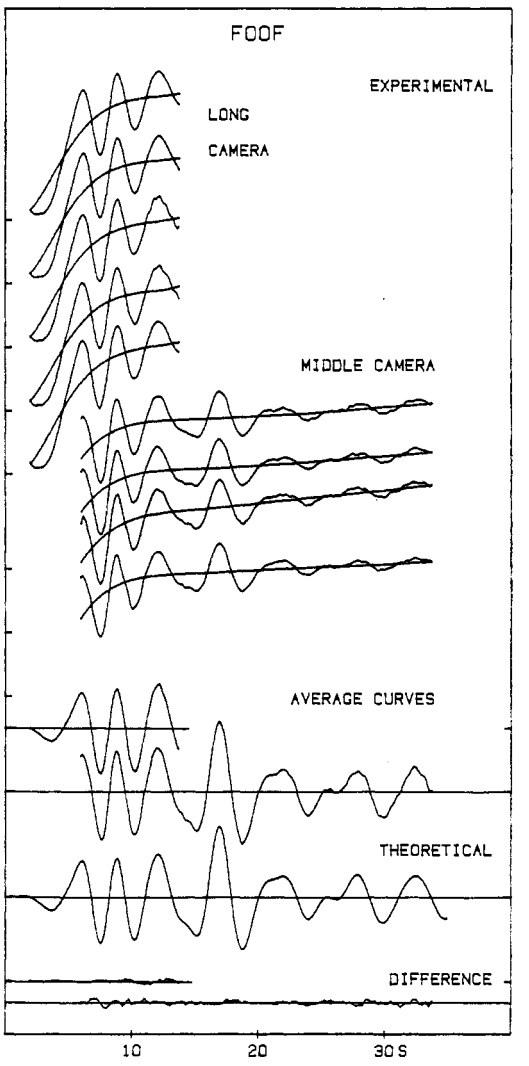


**Figure 1.** Intensity curves. The $s^4I_t(s)$ curves from each plate are shown superimposed on the final backgrounds and are magnified 5 times relative to the backgrounds. The theoretical curve is for model A of Table I. The difference curves are experimental minus theoretical.

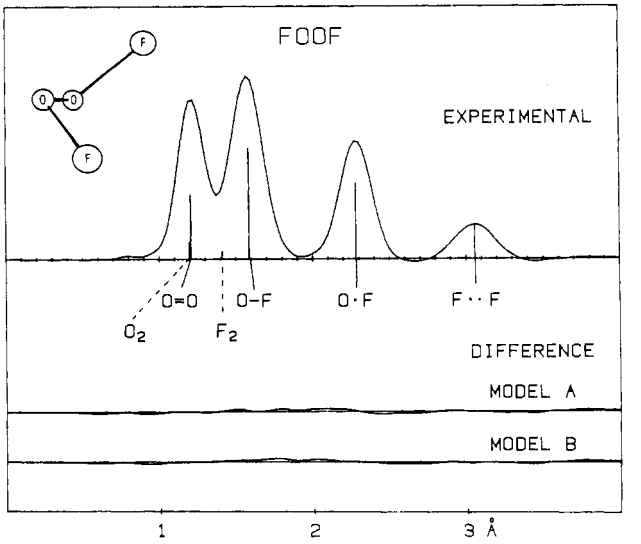


**Figure 2.** Radial distribution curves. The experimental curve was calculated from a composite of the average curves of Figure 1 with addition of theoretical data from model A for $s \le 2.00$ Å$^{-1}$.

(17) Gundersen, G.; Hedberg, K. *J. Chem. Phys.* **1969**, *51*, 2500.
(18) Hedberg, L. *Abstracts of Papers*, Fifth Austin Symposium on Gas Phase Molecular Structure, Austin, TX, March 1974; University of Texas: Austin, TX, 1974; p 37.
(19) The elastic amplitudes and phases were from: Schafer, L.; Yates, A. C.; Bonham, R. A. *J. Chem. Phys.* **1971**, *55*, 3055. The fluorine amplitudes were recalculated. Inelastic amplitudes used in the background removal were from: Cromer, D. T. *J. Chem. Phys.* **1969**, *50*, 4857.

**Table I.** Structural Results for $O_2F_2$[a]

| | model A[b,c] | | | | | model B[c,d] | model C[d,e] | | Jackson[f] |
|---|---|---|---|---|---|---|---|---|---|
| | $r_\alpha^0$, $\angle_\alpha$ | $r_g$[g] | $r_a$[g] | $l_{obsd}$ | $l_{calcd}$ | $r_\alpha^0$, $\angle_\alpha$ | $r_\alpha^0$, $\angle_\alpha$ | $l_{calcd}$ | $r_s$ |
| $r$(O=O) | 1.214 (2) | 1.216 | 1.215 | 0.046 (3) | 0.0411 | 1.213 (2) | 1.214 (2) | 0.0498 | 1.217 (3) |
| $r$(O—F) | 1.582 (2) | 1.586 | 1.583 | 0.069 (3) | 0.0621 | 1.580 (2) | 1.580 (2) | 0.0693 | 1.575 (3) |
| $r$(O···F) | 2.288 (3) | 2.291 | 2.289 | 0.073 (4) | 0.0702 | 2.286 (3) | 2.289 (3) | 0.0749 | |
| $r$(F···F) | 3.065 (4) | 3.068 | 3.064 | 0.113 (10) | 0.1136 | 3.059 (11) | 3.064 (4) | 0.1250 | |
| ∠OOF | 109.2 (2) | | | | | 109.1 (2) | 109.3 (2) | | 109.5 (5) |
| ∠FOOF | 88.1 (4) | | | | | 88.0 (9) | 87.9 (4) | | 87.5 (5) |
| $X(O_2)$[h] | 0.19 (2) | | | | | 0.19 (2) | 0.18 (2) | | |
| $X(F_2)$[h] | 0.09 (1) | | | | | 0.08 (1) | 0.09 (2) | | |
| MW/ED[i] | 400 | | | | | 0 | 400 | | |
| $\Delta A_z$[j] | −11.15 | | | | | 5.07 | −18.35 | | |
| $\Delta B_z$[j] | −4.03 | | | | | −23.61 | −6.25 | | |
| $\Delta C_z$[j] | −1.97 | | | | | −15.24 | −3.59 | | |
| $R$[k] | 0.063 | | | | | 0.058 | 0.070 | | |

[a] Distances ($r$) and amplitudes ($l$) are in angstroms; angles ($\angle$) are in degrees; rotational constant differences ($A$) are in megahertz. Quantities in parentheses are estimated $2\sigma$. [b] Preferred model. [c] Effects of vibration calculated from force field adopted for this work. [d] Observed amplitudes same as for model A. [e] Effects of vibration calculated from force field of ref 12. [f] Reference 5. [g] Uncertainties estimated to be the same as for $r_\alpha$. [h] Mole fractions. [i] Ratio of weighted squares of rotational constants to weighted squares of diffraction intensities. [j] Values are observed minus calculated values. [k] $R = [\sum_i w_i \Delta_i^2 / \sum_i w_i (s_i I_i(\text{obsd}))^2]^{1/2}$, where $\Delta_i = s_i I_i(\text{obsd}) - s_i I_i(\text{calcd})$.

**Table II.** Correlation Matrix (×100) for $O_2F_2$ Model A

| | | $\sigma$[a] | $r_1$ | $r_2$ | $r_3$ | $r_4$ | $\angle_5$ | $\angle_6$ | $X_7$ | $X_8$ | $l_9$ | $l_{10}$ | $l_{11}$ | $l_{12}$ |
|---|---|---|---|---|---|---|---|---|---|---|---|---|---|---|
| 1 | $r$(O=O) | 0.055 | 100 | −18 | <1 | −3 | −38 | 27 | −16 | 13 | 11 | −9 | 3 | 1 |
| 2 | $r$(O—F) | 0.044 | | 100 | −54 | 62 | −68 | 72 | −1 | −11 | −5 | −7 | 1 | −2 |
| 3 | $r$(O···F) | 0.059 | | | 100 | −3 | 86 | −85 | 1 | 6 | 4 | 4 | −1 | 3 |
| 4 | $r$(F···F) | 0.061 | | | | 100 | −26 | 46 | −3 | −5 | −2 | −5 | 1 | −1 |
| 5 | ∠OOF | 6.7 | | | | | 100 | −96 | 8 | 2 | <1 | 10 | −3 | 3 |
| 6 | ∠FOOF | 13.0 | | | | | | 100 | −6 | −4 | −1 | −9 | 2 | −3 |
| 7 | $X(O_2)$ | 0.92 | | | | | | | 100 | −83 | −63 | 40 | 9 | 2 |
| 8 | $X(F_2)$ | 0.68 | | | | | | | | 100 | 66 | −30 | −15 | −5 |
| 9 | $l$(O=O) | 0.102 | | | | | | | | | 100 | 7 | 18 | 7 |
| 10 | $l$(O—F) | 0.066 | | | | | | | | | | 100 | 36 | 12 |
| 11 | $l$(O···F) | 0.088 | | | | | | | | | | | 100 | 17 |
| 12 | $l$(F···F) | 0.332 | | | | | | | | | | | | 100 |

[a] Standard deviations (×100) from least squares. Distances ($r$) and amplitudes ($l$) are in angstroms; angles ($\angle$) are in degrees.

which require conversion from the $r_a$ type used to fit electron diffraction intensities; conversion of the $B_0$ rotational constants to $B_z$ is also required. Both types of conversions are calculated with use of a suitable force field.

Although force fields for $O_2F_2$ have been calculated in the course of earlier spectroscopic work[9-11] on the molecule, there have existed uncertainties about some of the assignments that have raised questions about some of the force constant values. The very recent spectroscopic study by Woodruff et al.[12] (hereafter WLSKJEK) appears to have resolved these assignment uncertainties, and the results of their normal-coordinate analysis have led these authors to propose a somewhat different force field. Because there are fewer independent observations (frequencies) than force constants in the complete quadratic force field for $O_2F_2$, the choice of force field is to some extent a matter of taste. WLSKJEK's choice has a large value for the O–O stretching constant and unusually large values for some of the off-diagonal constants; their preference is based on other correlations. Although the distance and rotational constant conversions required for our structure analysis are usually not very sensitive to reasonable changes in force constants, we decided it was necessary to verify the point for $O_2F_2$. Accordingly, we used our program ASYM20[20] to carry out a normal-coordinate analysis based on WLSKJEK's frequency assignments and selected a second force field that has a smaller value for the O–O stretching constant (with accompanying changes in some of the other constants). It is pleasing that the two force fields, which provide an equally good fit to the observed frequencies, also lead to similar distance and rotational constant corrections needed for our structure analysis. The values of WLSKJEK's and our symmetrized ($C_2$) constants and of the corresponding internal constants that may be calculated unambiguously from them are given in the supplementary material.

**Structure Refinement.** Refinement of the structure was carried out by least squares,[21] fitting simultaneously the averaged intensities from the two camera distances and the three rotational constants for the species $F^{16}O^{16}OF$ corrected to $B_z$ ($B_z = B_0 + \sum \alpha^{har}/2$). The $B_z$ values (in MHz) obtained with use of corrections from our force field, and in parentheses corrections from WLSKJEK's, were $A_z = 20266.18 - 109.39$ (95.24), $B_z = 5011.09 - 12.95$ (12.83), and $C_z = 4360.14 - 5.80$ (7.77); the conversion between rotational constants and moments of inertia was taken to be $B = 505379/I$). The structural parameters were chosen to be the bond distances $r$(O–O) and $r$(O–F), the bond angle ∠FOO, and the torsion angle $\tau$ = ∠FOOF. There are also four rms amplitude parameters, $l$, corresponding to the different interatomic distances. Because of the extreme thermal instability of $O_2F_2$ we included the mole fractions of $O_2$ and $F_2$ as parameters with distances and amplitudes kept at the values $r(O_2) = 1.2118$ Å, $l(O_2) = 0.0364$ Å, $r(F_2) = 1.412$ Å, and $l(F_2) = 0.0439$ Å. Test refinements of model systems that included the radical $O_2F$ were also carried out, but there was no indication of its presence, and in the final work it was assumed to be absent.

**Results.** Results for refinements of the structure of $O_2F_2$ under several sets of conditions are seen in Table I. Comparison of models A and C reveals the effect of vibrational corrections obtained from the two force fields discussed above; the differences between corresponding parameter values are negligible. The $r_\alpha^0$ columns of models A and B show the effect of inclusion of the rotational constants as auxiliary data in the refinement. Although the values of the quality-of-fit factor $R$ suggest a very slight inconsistency between the two types of data (the fit to the electron diffraction data is slightly better for model B), the differences

(20) Hedberg, L. *Abstracts of Papers*, Seventh Austin Symposium on Gas Phase Molecular Structure, Austin, TX, February 1978; University of Texas: Austin, TX, 1978; p 49.

(21) Hedberg, K.; Iwasaki, M. *Acta Crystallogr.* **1964**, *17*, 529.

between the parameter values themselves are regarded to be of no consequence. We take model A as "best model". Table II is the correlation matrix for model A.

## Discussion

Although the structures of $O_2F_2$ derived from our work and the microwave work are in good agreement (Table I), some small differences do exist. The differences may be attributed partly to the fact that the two methods lead to interatomic distances that are defined in different ways—in this case, a mixed $r_0/r_s$ type from microwave spectroscopy (since they were obtained from atomic coordinates calculated by joint use of isotopic substitution and center-of-mass conditions), and the usual $r_a$ type from electron diffraction.[22] In part the differences may also be due to uncertainty in the fluorine atom coordinates as deduced from the microwave spectrum: these atoms lie rather close (about 0.1 Å) to one of the inertial axes.

Our attempts to obtain data for the molecules $O_2F$ and/or $O_4F_2$ were unsuccessful. In none of our experiments did we find convincing evidence that we had generated identifiable amounts of these species, nor did we find evidence for the presence of $O_2F_2$ dimer or of an anti conformer of $O_2F_2$ itself. We are able, however, to draw some useful conclusions from these experiments. The results of run 6, which led to no discernible reaction, suggest that either (1) $O_2F_2$ and $O_2$ react to form $O_2F$ only very slowly compared to the transit time of the material through the gas nozzle (about 1.5 s) or (2) the equilibrium $O_2F_2 + O_2 = 2O_2F$ lies too far to the left to permit detection of $O_2F$ in our experiments.

The bonding in $O_2F_2$ with its short central and long peripheral bonds is clearly quite different from that in $N_2F_4$,[23] in which the distances correspond essentially to N–N and N–F single bonds and in which the internal rotation is only slightly restricted. Jackson[5] has discussed the bonding in $O_2F_2$ in terms of contributions from valence-bond structures of the type $F^-O{=}{}^+O{-}F$. These structures imply elongation of the F–O bonds and shortening of the O–O bond from the values found in $F_2O$ and in $H_2O_2$, respectively, in agreement with observation. The structure may also be rationalized from the molecular orbital point of view:[5] the two electrons assumed to occupy individually $\pi_y^*(2p)$ and a $\pi_z^*(2p)$ orbital on $O_2$ are respectively paired with electrons from fluorine atoms to form three-center bonds. The resulting picture accounts nicely for the bond lengths and torsion angle and for the relatively high barrier to internal rotation that is apparent from the narrowness of the F···F peak in our radial distribution curve. However, detailed theoretical calculations[13-16] indicate that the actual bonding picture is not so simple.

**Acknowledgment.** We gratefully acknowledge the valuable experimental assistance of L. B. Asprey, S. A. Kinkead, R. A. Kissane, and J. D. Purson of the Los Alamos National Laboratory. The Oregon State part of the work was supported by the National Science Foundation under grant CHE84-11165. The work at Los Alamos was done under the auspices of the U.S. Department of Energy.

**Registry No.** $O_2F_2$, 7783-44-0.

**Supplementary Material Available:** Tables III and IV, giving the internal and symmetrized ($C_2$) force constants, and Tables V–VII, giving the total scattered intensities from each plate, the calculated backgrounds, and the averaged intensities from each camera distance (13 pages). Ordering information is given on any current masthead page.

(22) Robiette, A. G. In *Molecular Structure by Diffraction Methods*; The Chemical Society: London, 1973; Vol. I, Chapter 4.

(23) See: Gilbert, M. M.; Gundersen, G.; Hedberg, K. *J. Chem. Phys.* **1972**, *56*, 1691 and other references cited therein.

Contribution from the Departments of Organic and Inorganic Chemistry, Royal Institute of Technology, S-100 44 Stockholm, Sweden, and Department of Structural and Inorganic Chemistry, Arrhenius Laboratory, University of Stockholm, S-106 91 Stockholm, Sweden

# Preparation and Characterization of New Transition-Metal Complexes of Dipyridylmethane Dicarboxylic Acids. Crystal Structure of the Copper(II) Complex of 1,1-Bis(6-carboxy-2-pyridyl)-1-methoxypropane

Ingeborg Csöregh,[1a] Björn Elman,[1b] Kerstin Högberg,[1c] Christina Moberg,*[1b] and Mats Nygren[1a]

*Received April 22, 1987*

The preparation of new complex-forming ligands of tetradental bis(picolinic acids), 1,1-bis(6-carboxy-2-pyridyl)alkanes, is described. These ligands are shown to readily form 1:1 complexes with $Cu^{2+}$, $Ni^{2+}$, $Co^{2+}$, $Zn^{2+}$, $Cd^{2+}$, and $Fe^{3+}$ ions and, provided they are lipophilic enough, to be versatile reagents for the extraction of these metal ions from an aqueous phase into an organic phase. The crystal and molecular structure of the tetrahydrate of the copper(II) complex of 1,1-bis(6-carboxy-2-pyridyl)-1-methoxypropane has been determined. The space group is monoclinic, $P2_1/n$, with $Z = 4$. The unit cell dimensions are $a = 11.5711$ (6) Å, $b = 7.7308$ (3) Å, $c = 21.7034$ (7) Å, and $\beta = 103.92$ (4)°. The final reliability index $R$ is 0.044 for 2785 reflections. The 1,1-bis(6-carboxy-2-pyridyl) moiety is slightly bent. The copper(II) ion is (4+1) coordinated in a nearly square-pyramidal arrangement. The distance from the copper to the "apex" oxygen, a hydrate O atom, is 2.244 (2) Å. The crystal structure is held together by a network of hydrogen bonds. Spectroscopic data indicate that the $N_2O_2$ atoms in the copper complex of 1,1-bis(6-carboxy-2-pyridyl)octene form a pseudotetrahedral arrangement, probably due to steric interactions between the side chain and a pyridine ring. The dehydration of precipitated metal complexes of 1,1-bis(6-carboxy-2-pyridyl)-1-methoxyalkanes as well as 4-(3-heptyl)pyridine-2-carboxylic acid has been monitored by means of TG and DSC measurements. Structural data combined with spectroscopic, TG, and DSC data are discussed in terms of the coordination around the metal ion.

## Introduction

To allow control of properties such as metal ion selectivity, it is of fundamental importance to design and prepare rigid ligands with appropriate donor atoms forced into desired positions. We are currently studying consequences of various substituents on the coordinating properties of pyridine- and quinolinecarboxylic acids and have found that groups influencing the stereochemistry and the electronic distribution of the ligands may have a pronounced effect on these properties.[2-5] To enable an understanding

(1) (a) University of Stockholm. (b) Department of Organic Chemistry, Royal Institute of Technology. (c) Department of Inorganic Chemistry, Royal Institute of Technology.

(2) Högberg, A. G. S.; Madan, K.; Moberg, C.; Sjöberg, B.; Weber, M.; Muhammed, M. *Polyhedron* **1985**, *4*, 971.

0020-1669/88/1327-0235$01.50/0 